Characterization of the lapis lazuli from the Egyptian treasure of Tôd and its alteration using external μ-PIXE and μ-IBIL

T. Calligaro, Y. Coquinot, L. Pichon, G. Pierrat-Bonnefois, P. de Campos, A. Re, D. Angelici, "Characterization of the lapis lazuli from the Egyptian treasure of Tôd and its alteration using external μ-PIXE and μ-IBIL", Nuclear Instruments and Methods in Physics Research B 318 (2014) 139-144
DOI 10.1016/j.nimb.2013.06.063

Characterization of the lapis lazuli from the Egyptian treasure of Tôd and its alteration using external µ-PIXE and µ-IBIL

T. Calligaro[(a)], Y. Coquinot[(a)], L. Pichon[(a,b)], G. Pierrat-Bonnefois[(c)], P. de Campos[(d)], A. Re[(e)], D. Angelici[(e,f)]

[(a)] Centre de Recherche et de Restauration des musées de France, Palais du Louvre, Paris, France

[(b)] Fédération de recherche NewAGLAE, FR3506 CNRS / Ministère de la Culture / UPMC, Palais du Louvre, 75001 Paris, France

[(c)] Musée du Louvre, Département des Antiquités Egyptiennes, Paris, France

[(d)] Institute of Physics, University of São Paulo, São Paulo, Brazil

[(e)] Università di Torino, Dipartimento di Fisica and Istituto Nazionale di Fisica Nucleare (INFN), Sezione di Torino, Torino, Italy

[(f)] Università di Torino, Dipartimento di Scienze della Terra, Torino, Italy

Corresponding author: thomas.calligaro@culture.gouv.fr

ABSTRACT

Lapis lazuli is among the earliest and most priced ornamental stone worked to produce carvings, beads and inlays as early as the 4th millennium BC. It is an heterogeneous rock composed of blue lazurite Na 3 Ca(Si 3 Al 3 O 12)S mixed with other minerals like calcite, diopside and pyrite. The historical source of lapis lazuli in antiquity is supposedly located in Afghanistan, in the Sar-e-Sang district, while other sources are known in Tajikistan and Russia (Baïkal area).

This work focuses on the lapis-lazuli of the Egyptian treasure of Tôd dated from Middle Kingdom (20th c. BC). Deposited in four copper boxes, it consists of thousands of blocks of raw lapis lazuli, minute fragments, beads and carvings stylistically dated to various periods. This discovery raises the question of the use of lapis lazuli in ancient Egypt because there is no source of lapis in this country. In addition, most of the lapis lazuli artefacts are strongly weathered. The aim of this work is to understand the alteration process and to verify if its provenance can still be determined.

A few artefacts were analysed using the new external microbeam line of the AGLAE facility of the C2RMF. The mineral phases were identified and corresponding trace elements (e.g. Ti, As, Ni, Ba) were ascribed using the quantitative PIXE elemental maps collected on the entire artefacts or on cross-sections. In parallel, the IBIL spectrum recorded for each point in the image provided an additional fingerprint of the luminescent phases, notably mineral species belonging to the cancrinite group. Most alteration products appeared to derive from the oxidation of the pyrite FeS 2 . It was observed that the alteration process extends to the core of most investigated artefacts. Despite such a strong alteration state, the chemical fingerprints recorded on the studied artefacts proved to be consistent with that of lapis lazuli from historical deposit of Badakshan, Afghanistan, previously investigated using the same l-PIXE/l-IBIL protocol.

1. Introduction

Among the earliest and most prized ornamental stone, lapis lazuli was used to produce carvings, beads and inlays since Neolithic times. The first lapis lazuli workshop excavated in Pakistan is dated from the 4th millennium [1] and its use in Mesopotamia and Ancient Egypt is largely attested since the 3rd millennium by the numerous artefacts adorned with this gemstone. From a mineralogical point of view, lapis lazuli is an heterogeneous metamorphic rock composed of minerals of the sodalite group such as lazurite Na 3 Ca(Si 3 Al 3 O 12)S – to which it owes its blue colour – intermixed with other whitish minerals like calcite, diopside, wollastonite and strewn with golden pyrite crystals. The main deposit of lapis lazuli exploited in Antiquity is located in Badakshan, Afghanistan while other sources are located in Tajikistan and Russia.

The determination of provenance of ancient lapis lazuli, a recurrent archaeological question, has motivated the development of many analytical approaches, from chemical analyses to IR spectroscopy [2]. Recently, Re [3–5] and Calligaro [6] and their coworkers have independently shown that most historical sources of lapis lazuli could be differentiated by the presence of particular mineral assemblages coupled with specific trace elements fingerprints.

The present work focuses on lapis-lazuli artefacts of the Egyptian treasure of Tôd, dating from Amenemhat II (1911–1876 BC), third king of the 12th dynasty, that was excavated in 1936 from the basement of a temple dedicated to the worship of Monthu, 30 km South of Luxor [7]. The treasure is shared between the Louvre museum in France and the Cairo museum in Egypt. Kept in four copper chests, it associates silver and gold with thousands of blocks of raw lapis lazuli, minute fragments, beads and carvings dated to the Middle Kingdom or earlier periods. According to their typology, the beads and amulets were made in Mesopotamia during the latter half of the 3rd millennium and the cylinder seals in the 3rd and early 2nd millennia. The treasure of Tôd represents

the largest set of ancient lapis lazuli left, after the corpus of lapis lazuli objects found in the royal tombs at Ur. It first raises the questions of the use of lapis lazuli in ancient Egypt and of the relations with Mesopotamia and the producing and manufacturing countries, because no source of lapis lazuli is known in Egypt. In addition, most lapis artefacts of the treasure present today a dull, whitish or brownish appearance (Fig. 1).

The issue addressed in this study is primarily to understand the alteration process that affected those lapis lazuli artefacts during their burial. The verification of the origin of the lapis is secondary, because the only source exploited at that time is probably the historical mines of Afghanistan. The copper boxes were recovered sealed in the basement of the temple, at level likely to be flooded by moments. The determination of the extent of the alteration state in the lapis lazuli artefacts and the understanding of the weathering process will be of considerable help for their preservation and to infer their original appearance. This weathering is not restricted to the lapis lazuli of the treasure of Tôd, as similar alterations have been observed on the lapis lazuli of other ancient objects from Egypt (Fig. 2). The analytical approach employed here is similar to the one applied previously to determine the provenance of lapis lazuli, i.e. the simultaneous combination of quantitative l-PIXE and l-ionoluminescence (IBIL) imagings.

2. Lapis lazuli samples

Eleven beads (Fig. 3) exhibiting characteristic alteration features seen on the other lapis lazuli artefacts were selected for this study. Three main type of structure of alteration were observed at the surface, whitish crystallizations, brown stained pyrite-rich areas (the pyrite turning in some samples to red) and microcrakings. Some beads are very weakly altered, showing only a slight bleaching while others present a very strong and deep alteration, from the surface up to the core of the bead. To assess the extent of the alteration inside the lapis lazuli, three beads exhibiting whitish, yellowish and brownish areas were cleaned in ultrasonic bath, cut and their cross-section polished at 2400 mesh with diamond solutions sample micro-pictures were taken at 20, 40 and 80X with a HIROX KH7700 digital microscope.

3. Experimental

To investigate the alteration of the lapis lazuli, we applied the same analytical approach that was previously developed for the determination of the provenance of the lapis-lazuli. The identification of the mineral phases was obtained using the quantitative PIXE elemental imaging capabilities coupled with IBIL of the new external microbeam line of the AGLAE facility at the C2RMF [8].

The 3-MeV proton beam was focused to 40-μm on the target. The scanning system combining a vertical magnetic scan of the beam over 640 μm with an horizontal target translation allowed to quickly acquire elemental maps on areas extending from 1.28 × 1.28 mm^2 to 3.2 × 3.2 mm^2 with a step size of 40 μm, i.e. from 32 × 32 to 80 × 80 pixels. PIXE data were acquired with five fast counting SDD X-ray detectors. As in our previous setup, one detector flushed with helium gas and protected from backscattered protons by a magnetic deflector was dedicated to measure low-Z (major) elements [9]. For the measurement of trace elements, the new system had four detectors to increase the statistics, which were screened with 100 μm Mylar absorbers to measure elements down to sulphur. With an intensity of about 2 nA, the counting rates were 5 k counts/s in the low energy detector to 150 k counts/s total in the trace detectors. The integrated charge was 2 nC per pixel, and so that the average time spend on each pixel was about 1 s for a total acquisition time of 15–100 min. The charge was monitored by recording silicon X-rays emitted by the Si 3 N 4 exit window with a dedicated SDD detector. The PYMCA program [10] was employed to rapidly extract maps of net peak areas, whereas more detailed information was gained by processing these raw maps using a TRAUPIXE [11], a home-made programme based upon GUPIX [12]. The derived quantitative concentration maps allowed to identify the mineral phases (e.g. lazurite, sodalite, pyrite, diopside, calcite) through their composition and to assign their corresponding trace element concentrations (e.g. Ti, As, Ni). The IBIL spectrum for each pixel was recorded using a 200–900 nm fiber optic spectrometer to provide an additional fingerprint for the luminescent mineral phases. The first objective was to identify the alteration products observed on the Egyptian artefacts. The second goal was to check if the provenance fingerprints can still be exploited, despite the alteration state of the artefacts. Indeed, the previous studies conducted on reference lapis lazuli samples of certified provenance have demonstrated that it is possible to distinguish the lapis lazuli sources (Chile, Russia, Tajikistan, Afghanistan) using PIXE and IBIL [3–6]. In addition, backscattering electrons (BSE) images from a scanning electron microscope (SEM) were employed to study details too small to be mapped in external beam (<40 μm). A few points were characterised by XRD with a micro diffractometer developed at the C2RMF. This equipment uses a copper X-ray tube Rigaku with a X-ray optics bringing a parallel beam of 30–200 μm on the sample. Diffraction patterns were recorded a 2D ‘‘imaging plate’’ Rigaku R-AXIS IV++ in 5–15 min, and the obtained circular 2D patterns were projected into linear ones. Corrections of the diffractograms and mineral phases identification were performed with the software EVA from Bruker.

4. Results

4.1. Altered lapis-lazuli

Alteration products resulting from the oxidation of the pyrite FeS 2 were identified. As seen in the quantitative PIXE maps (Fig. 4), the pyrite crystals appear surrounded by a layered structure. First, a few-micron wide iron oxide red layer, which can be observed by the increase of Fe content at the rim of the pyrite grains (increased Fe X-ray yield). A closer examination with SEM in BSE and EDX modes (Fig. 5) showed that the iron oxide layer (hematite or goethite) contains a layer of jarosite KFe 3 (SO 4) 2 (OH) 6 too thin to be visible in the PIXE maps but confirmed by XRD. Second, at long distance, the pyrite and its oxide layers are surrounded by relatively large patches of secondary minerals showing a white colour (enriched in Al, Si and O) and formed probably by the transformation of a mineral phase belonging to the sodalite group (lazurite). This peculiar zone looks whitish under the optical microscope (maybe due to micro-cracks) and emits an increased IBIL signal, possibly due to crystal damage. The sporadic presence of Cu observed in the maps correspond probably to the accumulation of copper compounds coming from the wall of the copper treasure box or from the decay of accompanying copper-based bronze artefacts. A few microns thick veins of white calcite (CaCO 3), neoformed, seen in the cracks result from the crystallization of jarosite and iron-oxides (goethite and hematite). Similar features were observed at the surface of the artefacts, plus a yellow crust that corresponds to sediment.

4.2. Non altered lapis-lazuli

The blue crystal grains are generally small (smaller than the 40 μm beam probe), as was confirmed by SEM images, and embedded in a whitish diopside matrix CaMgSi 2 O 6 . As it can be seen in S and Cl maps in Fig 4, the blue phase is mainly sodalite Na 8 Al 6 Si 6 O 24 Cl 2 (identified by the presence of Cl) and less often lazurite Na 3 Ca(Al 3 Si 3 O 12)S (presence of S). No wollastonite CaSiO 3 was found. The blue areas (lazurite and sodalite) bear a very low trace level of As (<300 lg/g). On the other hand, a rather high level of Ni (500–1000 lg/g) was measured in the pyrite crystals. The characteristic IBIL spectrum from a mineral phase of cancrinite group (narrow peaks between 400 to 600 nm) was recorded in a specific region (Fig. 6). The high Ca concentration determined by PIXE combined with S/Cl ratio around to 1:1 suggest a mineral phase belonging to the cancrinite group, possibly Afghanite of composition Na 22 Ca 10 (Si 24 Al 24)O 96 (SO4) 6 Cl 6 [13].

5. Discussion and perspectives

Most damage in the studied archaeological lapis lazuli can be ascribed to the oxidation of the FeS_2 pyrite crystals, which is known to be a very instable mineral in the presence of water or when placed in an oxidising environment [14]. The alteration often extends to the core of the artefacts, where pyrite crystals are partially altered, surrounded by a thin layer of goethite, hematite and sometimes jarosite. As a consequence, the artefact exhibit various yellow, brown to red mineral phases. Surprisingly no gypsum ($CaSO_4$) was observed despite the presence of Ca-containing phases. It means that Ca-rich phases as calcite or scapolite, identified in some lapis lazuli beads from the treasure of Tôd have not been altered. The sulphur resulting from the oxidation of FeS_2 might have escaped as SO_2 or the soluble sulphate salts might have been leached out by the fluids, in particular if the copper boxes have been flooded. The volume expansion of oxidation compounds from the pyrite decay explains the cracks observed in some samples. The circulation of the fluids and the dissolution of certain phases inside the artefacts have sometimes left profound crevices. In conclusion, the lapis-lazuli of the treasure of Tôd has lost their original appearance. The artefacts had likely a brighter blue colour, while their present appearance is rather that of low grade, greyish and dotted lapis lazuli. This study has opened new issues and calls for new investigations. The precise characterisation of the iron (hydr)oxide layer surrounding the weathered pyrite would need further investigation with complementary methods (e.g. by µ-Raman spectrometry or l-XRD). The presence of hematite, not reported in previous pyrite decay studies, calls for a more thorough study of pyrite alteration in a long-term burial environment.

On the other hand, the recorded fingerprint appeared still exploitable for provenancing the lapis lazuli. The presence of diopside, of lazurite and sodalite bearing low As concentrations, of pyrite containing high Ni traces, of Afghanite and the absence of wollastonite and of Ba traces constitutes a fingerprint compatible with that of lapis lazuli from Afghanistan, as reported in [4] and [6]. However, only eleven artefacts among the thousands of the treasure of Tôd have been investigated yet. It would be interesting to analyse more samples. Indeed, the comparison of the fingerprints of various typological classes of artefacts (stylistic/dating) could reveal a more detailed picture.

In addition, in this study we have applied a promising statistical method called Non-Negative Matrix Approximation (NNMA) [15] or Positive Matrix Factorization (PMF) by other authors, which is implemented in the PYMCA program, in view to simplify data mining of the numerous quantitative composition maps delivered by PIXE. The NNMA multivariate method has a similar objective as the well-known principal components analysis (PCA), namely data reduction, with the notable difference that all eigen values calculated are positive, thus producing results easier to interpret from a mineralogical viewpoint. Fig. 7 shows the eigen maps and eigenvectors derived on

the same data as in Fig. 4. The first four components automatically generated directly correspond to main mineral phases in the sample, i.e. diopside, sodalite, pyrite and calcite. This approach opens new perspectives for the automated processing of the increasing data generated by PIXE mapping, in particular for mineral phases identification in rocks and ceramics.

Acknowledgements

We acknowledge the skilful operation of AGLAE by B. Moignard and Q. Lemasson and the constant help of C. Pacheco. We are indebted to JC Dran for his enthusiastic support and highlighting scientific discussions. We thank the Ville de Paris for its financial support to the development of the New AGLAE project. This work is realized in the framework of the Equipex Project New AGLAE (‘‘Investissements d’avenir’’ program) and with the financial support from the French Government through the grant from the Agence Nationale de la Recherche ANR-10-EQPX-22. The travel expenses for A. Re and D. Angelici have been funded by the INFN experiment ‘‘FARE’’.

References

[1] M. Vidale, M. Tosi, Paléorient 16 (1990) 89.

[2] M. Bacci, C. Cucci, E. Del Federico, A. Ienco, A. Jerschow, J. Newman, M. Picollo, Vib. Spectrosc. 49 (2009) 80.

[3] A. Re, D. Angelici, A. Lo Giudice, E. Maupas, L. Giuntini, S. Calusi, N. Gelli, M. Massi, A. Borghi, L.M. Gallo, G. Pratesi, P.A. Mandò, Appl. Phys. A 111 (2013) 69.

[4] A. Lo Giudice, A. Re, S. Calusi, L. Giuntini, M. Massi, P. Olivero, G. Pratesi, M. Albonico, E. Conz, Anal. Bioanal. Chem. 395 (2009) 2211.

[5] A. Re, A. Lo Giudice, D. Angelici, S. Calusi, L. Giuntini, M. Massi, G. Pratesi, Nucl. Instr. Meth. B269 (2011) 2373.

[6] T. Calligaro, Y. Coquinot, L. Pichon, B. Moignard, Nucl. Instr. Meth. B269 (2011) 2364.

[7] G. Pierrat-Bonnefois, Le lapis lazuli du trésor de Tod, in Les pierres précieuses de l’Orient ancien, Dossiers du musée du Louvre, éditions de la Reunion des musées nationaux 1995, Paris.

[8] L. Pichon, Q. Lemasson, B. Moignard, C. Pacheco, Ph. Walter, these proceedings.

[9] T. Calligaro, J.-C. Dran, E. Ioannidou, B. Moignard, L. Pichon, J. Salomon, Nucl. Instr. Meth. B161 (163) (2000) 328.

[10] V.A. Solé, E. Papillon, M. Cotte, Ph. Walter, J. Susini, Spectrochim. Acta B62 (2007) 63.

[11] L. Pichon, L. Beck, Ph. Walter, B. Moignard, T. Guillou, Nucl. Instr. Meth. B268 (2010) 2028.

[12] J.A. Maxwell, J.L. Campbell, W.J. Teesdale, Nucl. Instr. Meth. B43 (1989) 218.

[13] D.D. Hogarth, Can. Mineral. 17 (1979) 47.
[14] J. Rimstidt, D. Vaughan, Geochim. Cosmochim. Acta 67 (2003) 873.
[15] D.D. Lee, H.S. Seung, Nature 401 (1999) 788.

Figures

Fig. 1. Some lapis lazuli artefacts from the treasure, mostly pierced beads. Note their strong alteration.

Fig. 2. Altered Egyptian carving (Louvre Museum) showing red mineral crystals scattered at the surface. (For interpretation of the references to colour in this figure legend, the reader is referred to the web version of this article.)

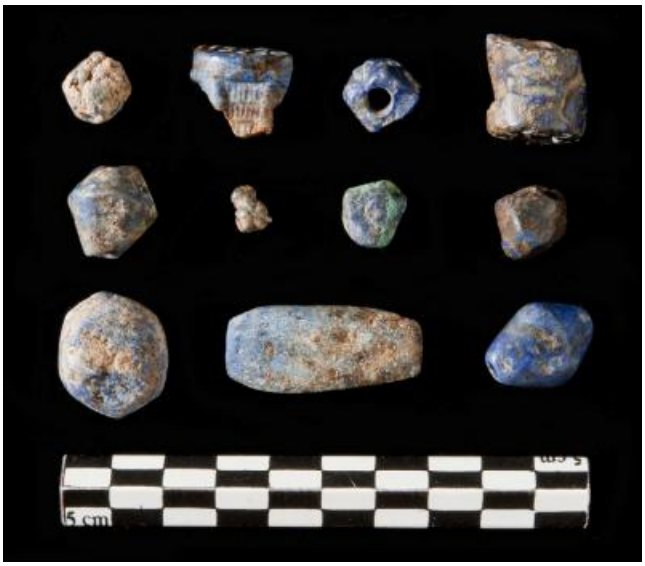

Fig. 3. Eleven studied artefacts: beads, seal-cylinders, carvings. The maps presented here are from sample E15280A-13-3 (2nd row, 1st column) and E15280A-138 (2nd row, 4th column). Note the miniature hippo head in 2nd row, 2nd column. Various whitish, brownish and greenish alterations can be observed at the surface. (For interpretation of the references to colour in this figure legend, the reader is referred to the web version of this article.)

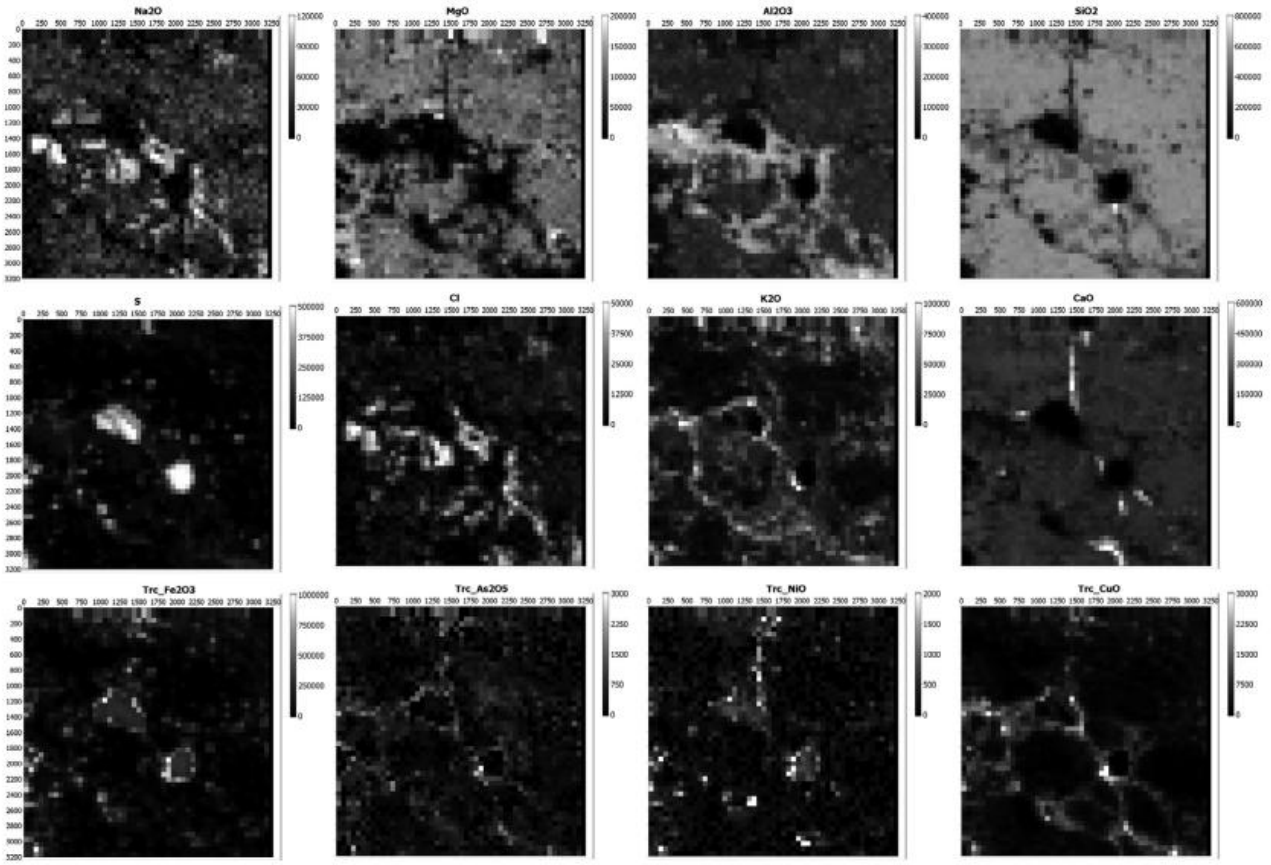

Fig. 4. Quantitative PIXE elemental maps obtained on sample E15280A-13-8A cross-section allowing mineral phases identification. Axes are labelled in µm, greyscale levels are in ug/g.

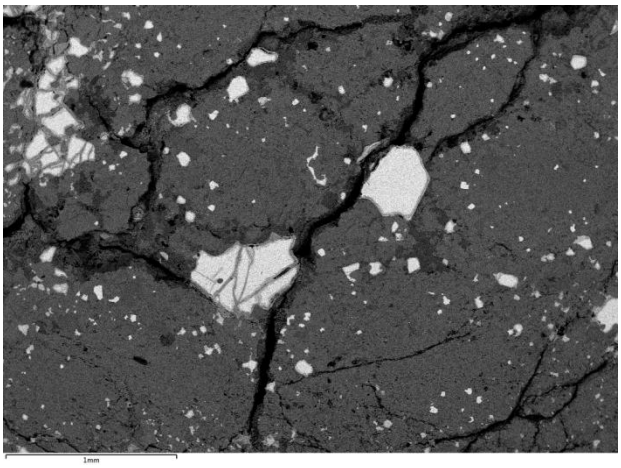

Fig. 5. Backscattering electron image of the same region as in Fig. 4 obtained with SEM. Note the thin iron oxide layer (grey) surrounding the pyrite grains (white).

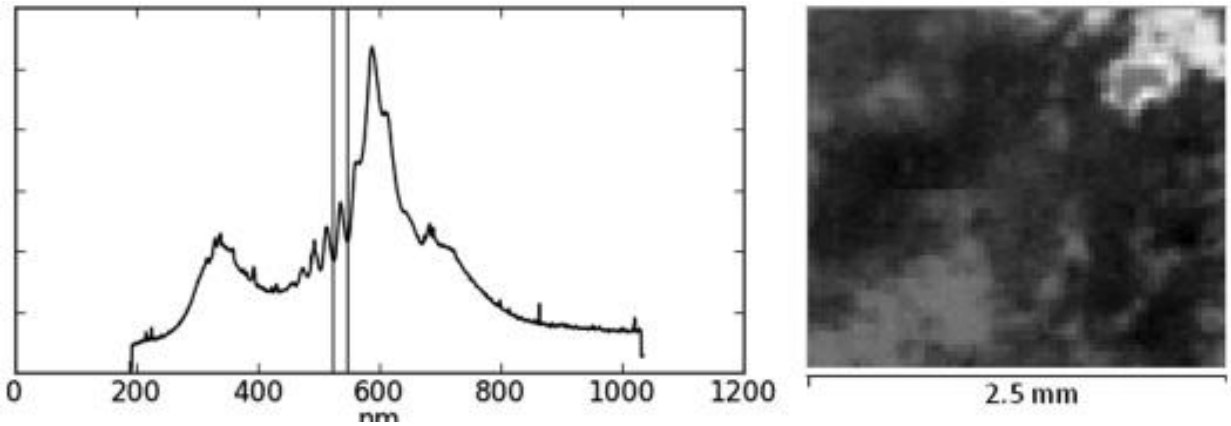

Fig. 6. Left, IBIL spectrum recorded in the upper left region in sample E15280A-13-3. Narrow peaks in the 400–600 nm are typical of a phase of the cancrinite group, possibly Afghanite, according to the composition obtained by PIXE. Right is the map of the 505–252 nm band in the scanned region.

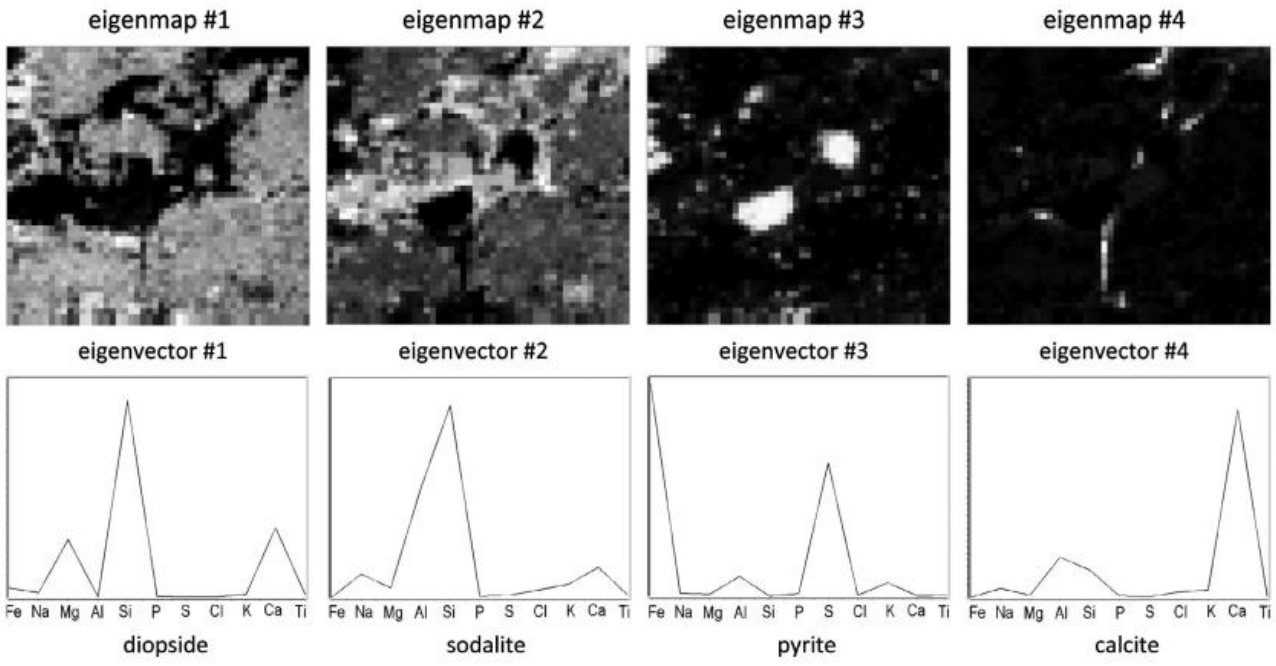

Fig. 7. Output of the Non-Negative matrix approximation applied to the concentration maps recorded on E15280A-13-8A cross-section. In the up row are the first four eigenmaps generated by algorithm. In the bottom row are the corresponding eigenvectors in relative elemental concentration that can be interpreted as the main mineral phases present in the lapis-lazuli sample: diopside CaMgSi 2 O 6 , sodalite Na 8 Al 6 Si 6 O 24 Cl 2 , pyrite FeS 2 and calcite CaCO 3 (bottom labels).